Solid State Communications, Vol. 82, No. 3, pp. 183–187, 1992.
Printed in Great Britain.

0038-1098/92 $5.00 + .00
Pergamon Press plc

ON THE PHENOMENOLOGY OF THE INFRARED PROPERTIES OF THE COPPER-OXIDE SUPERCONDUCTORS

D.B. Romero,* C.D. Porter and D.B. Tanner

Department of Physics, University of Florida, Gainesville, FL 32611, USA

L. Forro, D. Mandrus and L. Mihaly

Department of Physics, SUNY, Stony Brook, NY 11794, USA

G.L. Carr

Grumman Corporate Research Center, Bethpage, NY 11714, USA

and

G.P. Williams

National Synchrotron Light Source, BNL, Upton, NY 11973, USA

(*Received* 18 *September* 1991 *by M.F. Collins*)

The temperature dependent infrared conductivities of $Bi_2Sr_2CaCu_2O_8$ ($T_c \simeq 82$ K) and $Bi_2Sr_2CuO_6$ ($T_c \lesssim 5$ K) are compared with non-Fermi liquid approaches to the normal state of the high T_c superconductors. We find reasonable agreement with our data only for $\omega \lesssim 0.12$ eV. We attribute the remaining spectral weight to a low-energy excitation in copper-oxide superconductors doped well above the metal–insulator transition.

THE HIGH T_c superconductors (HTSC) have normal state properties that are almost as interesting as the superconductivity. Several workers have suggested that the observed normal state properties of the HTSC manifest non-Fermi liquid character [1, 2] – either a marginal Fermi liquid [2] (MFL) or a Luttinger liquid [1]. Directly relevant to infrared measurements is the temperature (T) and frequency (ω) dependence of the scattering rate (τ^{-1}) of the charge carriers: the non-Fermi liquid theories predict that $\tau^{-1} \propto \max[T, \omega]$. In the MFL proposed by Varma *et al.* [2], this behavior may arise from scattering of the free carriers by a spectrum of particle–hole excitations in which the low-energy scale is set by the temperature. The nested Fermi liquid theory of Virosztek and Ruvalds [3] gives also $\tau^{-1} \propto \max[T, \omega]$ for the scattering rate. This differs from ordinary metallic behavior, where $\tau^{-1} \propto \max[T^2, \omega^2]$ for the case of electron–electron scattering, τ^{-1} = constant for electron-impurity scattering and $\tau^{-1} \propto T$ at high T and low ω, with characteristic power laws in T and ω-dependent Holstein sidebands at lower T, for electron–phonon scattering.

The normal state infrared conductivity of the HTSC is Drude-like in the far-infrared whereas substantial non-Drude conductivity persists at higher frequencies [4–9]. Both dc-transport [10, 11] and far-infrared [4–7] data reveal that $\tau^{-1} \propto T$. Conventional analysis [4, 7, 10] of these data, based on electron-phonon scattering, obtains a coupling of moderate strength ($\lambda < 1$). In contrast, a larger coupling constant ($\lambda > 1$) is needed for the non-Drude conductivity at higher frequencies within such an approach [7].

In this paper, we will compare the T-dependence of the infrared conductivity of $Bi_2Sr_2CaCu_2O_8$ ($T_c \simeq 82$ K) and $Bi_2Sr_2CuO_6$ ($T_c \lesssim 5$ K) with predictions of the non-Fermi liquid theories. These materials are ideal candidates for such study since they show the unconventional characteristic linear-T variation of the in-plane resistivity (ρ_{ab}) [11]. Also, because these bismuth based copper-oxide superconductors contain Cu–O chains, their infrared conductivities is expected to be solely due to the intrinsic dynamics of the CuO_2 planes.

We measured the transmittance ($\mathcal{T}$) of free-standing single crystals of $Bi_2Sr_2CaCu_2O_8$ (2212) and $Bi_2Sr_2CuO_6$ (2201) over a wide range of frequency ($80 \leqslant \omega \leqslant 35000\,\mathrm{cm}^{-1}$) and at several temperatures (T = 10–300 K) [5, 6]. The ω-dependent conductivity was determined by Kramers–Kronig analysis of

* Present address: Department of Physics, Virginia Tech, Blacksburg, VA 24061 USA.

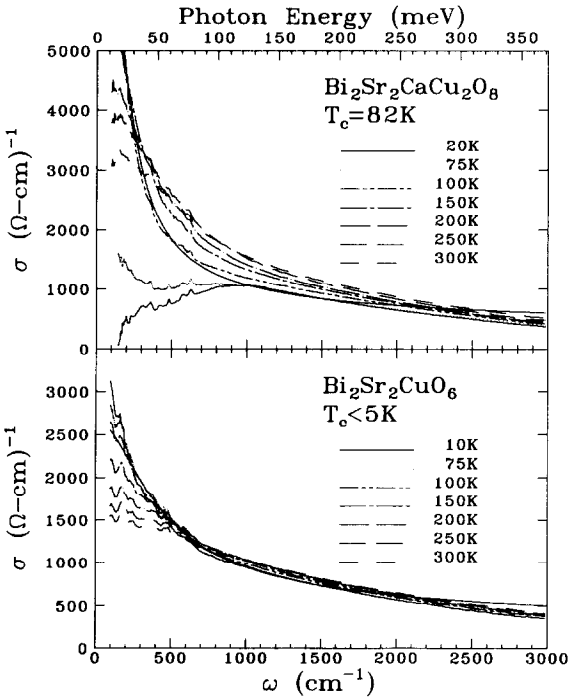

Fig. 1. Temperature dependence of the conductivity of $Bi_2Sr_2CaCu_2O$ and $Bi_2Sr_2CuO_6$.

$\mathcal{T}$. The complex transmission amplitude is $t(\omega) = \sqrt{\mathcal{T}(\omega)}\exp(i\theta(\omega))$ where $\mathcal{T}(\omega)$ is the measured transmittance and $\theta(\omega)$ is the phase shift upon transmission, which is related to $\mathcal{T}$ by a Kramers–Kronig integral, just like reflectance. Once the phase shift θ is known, the complex refractive index can be obtained by numerical solution of,

$$\sqrt{\mathcal{T}}\exp(i\theta) = \frac{4N}{(N+1)^2\exp(-i\delta) - (N-1)^2\exp(i\delta)},$$

where $N = \sqrt{\varepsilon}$ is the complex index of refraction, with $\varepsilon = \varepsilon_1 + 4\pi\sigma_1/\omega$ the complex dielectric function, and $\delta = \omega Nd/c$ the complex phase shift introduced by the film. An added complication is that the phase shift which the radiation would have travelling through a thickness d of vacuum ($\omega d/c$) has to be added to θ prior to solving the above equation for N. For extrapolations, we used a power law approach to $\mathcal{T} = 1$ at high frequencies and $\mathcal{T} = a + b\omega^2$ for $T > T_c$ and $\mathcal{T} = b\omega^2$ for $T < T_c$ at low frequencies.

Results of Kramers–Kronig analysis of the transmittance data are given in Fig. 1, which shows for both samples $\sigma_1(\omega)$ at several temperatures over 80–3000 cm^{-1}. In the normal state, the low-frequency conductivity approaches the d.c. conductivity and falls with increasing frequency in a way consistent with the Drude response of free carriers. However, at higher frequencies, the decrease in the conductivity is closer to ω^{-1} than the ω^{-2} behavior expected for Drude free carriers. Furthermore, the T-dependence of $\sigma_1(\omega)$ at high frequencies is much smaller than at d.c. or low frequencies. This is the "non-Drude" conductivity [4–9] that is a well known property of the high T_c superconductors.

Below T_c, for the 2212 sample, much of the free carrier oscillator strength goes into the superconducting condensate. The remaining infrared absorption appears to have an onset near $\omega = 150\,\text{cm}^{-1}$, with some weak structure in the phonon region. In contrast to reported results [8] for untwinned single crystals of $YBa_2Cu_3O_7$, we observe finite absorption well below $\omega \simeq 500\,\text{cm}^{-1}$ in the 2212 sample.

To analyze our data, we used an expression for the conductivity derived by Littlewood and Varma [12] from their marginal Fermi liquid theory. The conductivity is,

$$\sigma(\omega) \simeq \frac{i\omega_p^2/4\pi}{\omega - 2\Sigma(\omega/2)}, \quad (1)$$

where ω_p is the plasma frequency and Σ is the quasi-particle self-energy which is given by:

$$\Sigma_{\text{MFL}}(\omega, T) = 2\lambda\omega\log\left(\frac{\pi T - i\omega}{\omega_c}\right) - i\pi^2\lambda T. \quad (2)$$

Here λ is a coupling constant and ω_c is a high frequency cutoff. The limiting cases for Σ_{MFL} yields $-\text{Im}(\Sigma_{\text{MFL}}) = \pi^2\lambda T$ for $\omega \ll T$ and $-\text{Im}(\Sigma_{\text{MFL}}) = \pi\lambda\omega$ for $\omega \gg T$, which are the appropriate non-Fermi liquid behavior for the quasi-particle damping. We included an elastic scattering term (Σ_i) in the self-energy expression to account for any residual resistivity caused by impurities. Thus, we used $\Sigma = \Sigma_{\text{MFL}} - i\Sigma_i$.

The data shown in Fig. 1 were fitted to equations (1) and (2). We obtain good fits to the conductivity, as indicated by the thin solid lines in Fig. 1 for $T = 100$ K. The main discrepancy is that the calculation falls below the experiment at around 500 cm^{-1} and rises above it for $\omega \gtrsim 2000\,\text{cm}^{-1}$. This excess high frequency conductivity is a consequence of equation (2) yielding $-\text{Im}\,\Sigma \propto \omega$ at high frequencies whereas the data would give $-\text{Im}\,\Sigma \simeq$ constant. Note, however, that this discrepancy occurs well above ω_c. Our model calculation yielded $\omega_c \simeq 1208\,\text{cm}^{-1}$ for both materials; $\Sigma_i \simeq 0$ for 2212 and $\Sigma_i \simeq 328\,\text{cm}^{-1}$ for 2201. In Table 1, we show the values for ω_p and λ. ω_p is essentially constant ($\omega_p = 14\,700 \pm 400\,\text{cm}^{-1}$ for 2212 and $\omega_p = 12\,800 \pm 100\,\text{cm}^{-1}$ for 2201) in agreement with values determined from the sum rule. The characteristic coupling constant, $\lambda = 0.27 \pm 0.02$ for

Table 1. Parameters for marginal Fermi liquid fit to $\sigma_1(\omega)$

T (K)	$Bi_2Sr_2CaCu_2O_8$		$Bi_2Sr_2CuO_6$	
	ω_p (cm^{-1})	λ	ω_p (cm^{-1})	λ
10			12610	0.272
25			12680	0.267
50			12700	0.269
75			12840	0.266
100	13950	0.244	12770	0.267
125			12820	0.267
150	14710	0.279	12840	0.269
175			12830	0.270
200	14870	0.277	13020	0.287
250	15060	0.261	12920	0.278
300	14910	0.259	12940	0.270

both materials, is also in accord with results from transport [10] and far-infrared measurements [4, 7].

A more direct test of the MFL theory is to compare the calculated and measured $-\mathrm{Im}\,\Sigma$ and $m_{\mathrm{eff}}/m_b \equiv 1 - \mathrm{Re}\,\Sigma/\omega$. Using equation (1) we can calculate these two quantities from the Kramers–Kronig derived optical constants. In these calculations, shown in Fig. 2 (for 2212) and Fig. 3 (for 2201), we used the values for ω_p from Table 1.

The calculated and experimentally derived forms

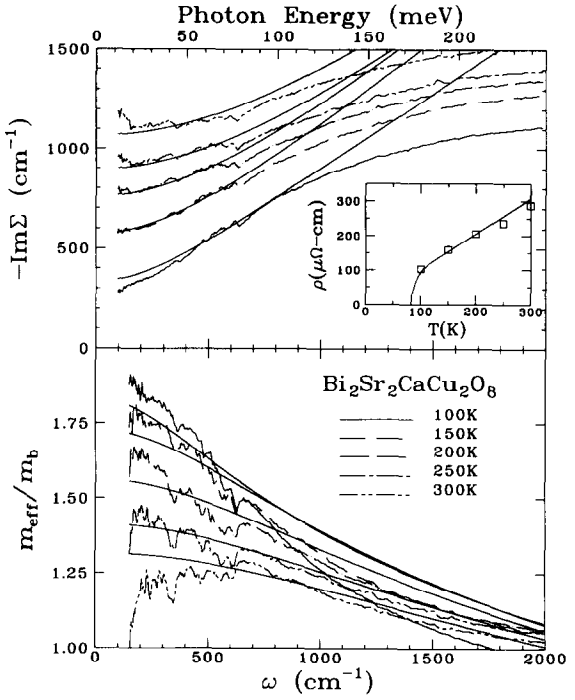

Fig. 2. Frequency dependent damping and effective mass at several temperatures for $Bi_2Sr_2CaCu_2O_8$.

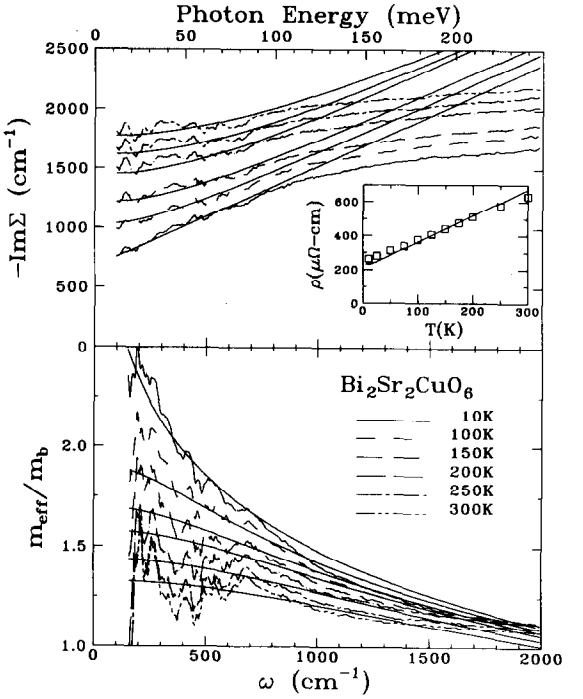

Fig. 3. Frequency dependent damping and effective mass at several temperatures for $Bi_2Sr_2CuO_6$.

for $-\mathrm{Im}\,\Sigma$ and m_{eff}/m_b agree in some important ways, particularly below ω_c. Both yield a d.c. resistivity that is in accord with the measured ρ_{dc}, as shown in the insets of Figs. 2 and 3. There is an increasing $-\mathrm{Im}\,\Sigma$ at higher frequencies. The effective mass is enhanced at lower frequencies by an amount which is largest at lower temperatures.

There are, however, also some qualitative differences. First, the cutoff frequency ($\omega_c = 0.15$ eV) is relatively low. (In fact, the good agreement of the fits to our data is limited to below $\omega \simeq 1000\,\mathrm{cm}^{-1} = 0.12$ eV.) This implies that at the higher temperatures, true MFL behavior (i.e., $T \ll \omega_c$) is not really achieved. This low cutoff is also difficult to understand in view of the high cutoff ($\omega_c \geq 0.5$ eV) suggested by Raman [13] and photoemission [14] experiments. Second, the experimental $-\mathrm{Im}\,\Sigma$ curves level off above ω_c whereas the calculated ones continue in a straight line. Third, the data in Figs. 2 and 3 show that $m_{\mathrm{eff}}/m_b(\omega = 0)$ decreases linearly with T, while the calculation predicts a more gradual logarithmic decrease.

Therefore, the limited frequency range in which the non-Fermi liquid model is valid would imply that not all of the midinfrared spectral weight can be assigned to these carriers. This conclusion is clearly illustrated in Fig. 4 where we show the $T = 100$ K effective number of carriers per CuO_2 unit for the two samples. Note that N_{eff} assumes its full value (0.3 per

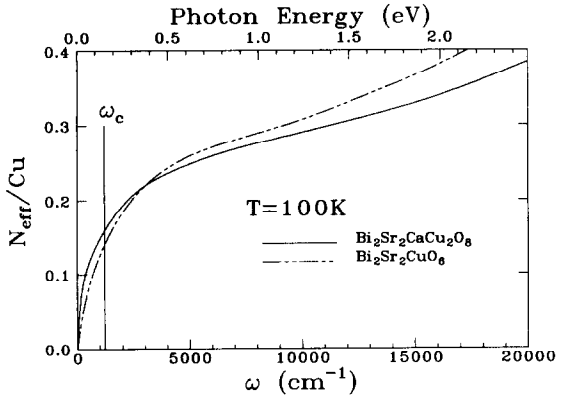

Fig. 4. Effective number of free carriers per CuO_2 unit for $Bi_2Sr_2CaCu_2O_8$ and $Bi_2Sr_2CuO_6$. ω_c indicates the frequency cutoff in the marginal Fermi liquid analysis.

Cu atom for both 2212 and 2201) at frequencies much higher than ω_c. Thus, approximately half of the midinfrared spectral weight lies above ω_c.

We now turn our attention to the infrared conductivity below T_c. The conductivity below T_c of the 2212 sample, shown in Fig. 1, is not zero for $\omega \gtrsim 150\,\mathrm{cm}^{-1}$. What is currently emerging to be an intrinsic property of the cuprates is the observation [15, 16] of this finite absorption down to the lowest measurable frequencies. Clearly, this is another experimental constraint to any theory of the high T_c superconductivity. Calculation [12, 17] of the frequency dependent conductivity for a superconductor within the marginal Fermi liquid model predicts the onset of optical absorption, in the clean limit, begins at 4Δ not at 2Δ. The reason is that for absorption to occur, the photon energy must be sufficient (a) to break a Cooper pair (2Δ) and (b) to create a charge or spin fluctuation (also 2Δ), for a total of 4Δ. The implication of this prediction to an observed peak in $\mathscr{T}_S/\mathscr{T}_N$ for the 2212 sample was discussed in an earlier work [6]. With regards to the non-zero absorption at low frequencies, it could come from direct absorption by the excitations which scatter the carriers [2, 12]. An interesting possibility [16] is that the finite absorption is due to some type of collective excitation to excited states of the Cooper pair below the superconducting gap.

An alternate point of view [4, 5, 7] is to attribute this finite absorption below T_c to the presence of a low-energy excitation, distinct from the free-carriers, in the infrared conductivity. This midinfrared absorption would also be reponsible for much of the non-Drude character of the conductivity above T_c. In this two-component model, there are two types of carriers: free carriers (with, conceivably, dynamics that are consistent with non-Fermi liquid behavior) and bound carriers (which are not superconducting). Possible evidence for the presence of two types of carriers in the CuO_2 plane comes from infrared and Hall effect measurements. The total in-plane spectral weight, deduced from the analysis of infrared data, is constant for all temperatures while the Hall coefficient [11], which determines the number of free carriers in a one-component picture, is strongly T-dependent. The presence of two types of carriers can reconcile these results.

In our previous [6] two-component analysis of $\mathscr{T}$ for the 2212 sample, we observe that the contribution centered near $\omega \simeq 1000\,\mathrm{cm}^{-1}$ showed a weak T-dependence of the peak position and its width, with the latter increasing nearly linear in T. Interestingly, a similar T-dependence of a peak near $\omega \simeq 1000\,\mathrm{cm}^{-1}$ was also observed [18] in lightly doped insulating samples of Nd_2CuO_{4-y}. If this excitation is reponsible for the linear T-dependent damping of the free carriers, then it suggests two important implications in the microscopic theory of the HTSC: (1) the excitation which determines the dynamics of the HTSC is optically active and (2) it may provide a link between antiferromagnetism and superconductivity (if it is indeed an excitation which persists in both the metallic and insulating state).

In conclusion, we have shown that a non-Fermi liquid description of free carrier dynamics in the HTSC is limited to a narrow range of frequency ($\omega \gtrsim 0.12\,\mathrm{eV}$). The remaining spectral weight, *not due to free carriers*, is attributed to a low-energy excitation which persists in copper-oxide materials doped well above the metal-insulator transition. The presence of this bound-state excitation can also account for the intrinsic finite absorption below T_c.

Acknowledgements – Research at Florida is supported by DARPA grant MDA-972-88-J-1006. Research at Stony Brook is supported by NSF grant DMR9016456. NSLS is supported by DOE through contract DE-AC02- 76CH00016. We thank G.A. Thomas, T. Timusk, P.B. Littlewood, and C.M. Varma for useful discussions.

REFERENCES

1. See the article by P.W. Anderson in *Strong Correlation and Superconductivity*, (Edited by H. Fukuyama, S. Maekawa and A.P. Malozemoff), Springer, New York (1989).
2. C.M. Varma, P.B. Littlewood, S. Schmitt-Rink, E. Abrahams & A. Ruckenstein, *Phys. Rev. Lett.* **63,** 1996 (1989).
3. A. Virosztek & J. Ruvalds, *Phys. Rev.* **B42,** 4064 (1990).
4. K. Kamaras, S.L. Herr, C.D. Porter, N. Tache, D.B. Tanner, S. Etemad, T. Venkatesan,

E. Chase, A. Inam, X.D. Wu, M.S. Hedge & B. Dutta, *Phys. Rev. Lett.* **64,** 84 (1990).
5. L. Forro, G.L. Carr, G.P. Williams, D. Mandrus & L. Mihaly, *Phys. Rev. Lett.* **65,** 1941 (1990).
6. D.B. Romero, G.L. Carr, D.B. Tanner, L. Forro, D. Mandrus, L. Mihaly & G.P. Williams, *Phys. Rev.* **B44,** 2818 (1991).
7. J. Orenstein, G.A. Thomas, A.J. Millis, S.L. Cooper, D.H. Rapkine, T. Timusk, L.F. Schneemeyer & J.V. Waszczak, *Phys. Rev.* **B42,** 6342 (1990).
8. Z. Schlesinger, R.T. Collins, F. Holtzberg, C. Field, U. Welp, G.W. Crabtree, Y. Fang & J.Z. Liu, *Phys. Rev. Lett.* **65,** 801 (1990).
9. S.L. Cooper, G.A. Thomas, J. Orenstein, D.H. Rapkine, M. Capizzi, T. Timusk, A.J. Millis, L.F. Schneemeyer & J.V. Waszczak, *Phys. Rev.* **B40,** 11358 (1989).
10. M. Gurvitch & A.T. Fiory, *Phys. Rev. Lett.* **59,** 1337 (1987).
11. L. Forro, D. Mandrus, C. Kendziora, L. Mihaly & R. Reeder, *Phys. Rev.* **B42,** 8704 (1990).
12. P.B. Littlewood & C.M. Varma, *J. Appl. Phys.* **69,** 4979 (1991).
13. See the article by M.V. Klein in *Laser Optics of Condensed Matter*, (Edited by A.A. Maradudin, E. Garmire & K.K. Rebane), Plenum, New York (1990).
14. C.G. Olson, R. Liu, D.W. Lynch, R.S. List, A.J. Arko, B.W. Veal, Y.C. Chang, P.Z. Jiang & A.P. Paulikas, *Phys. Rev.* **B42,** 381 (1990).
15. M. Quijada, D.B. Romero, D.B. Tanner, J.P. Rice & D.M. Ginsberg, to be published.
16. T. Pham, M.W. Lee, H.D. Drew, U. Welp & Y. Fang, *Phys. Rev.* **B44,** 5377 (1991).
17. E.J. Nicol, J.P. Carbotte & T. Timusk, *Phys. Rev.* **B43,** 473 (1991).
18. G.A. Thomas, D.H. Rapkine, S.L. Cooper, S.W. Cheong & A.S. Cooper, *Phys. Rev. Lett.* **67,** 2906 (1991).